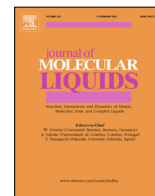




Contents lists available at ScienceDirect

Journal of Molecular Liquids

journal homepage: www.elsevier.com/locate/molliq

A study of the interactions between ephedrine and human serum albumin based on spectroscopic, electrochemical and docking assessments

Sedigheh Hashemnia^{a,*}, Fatemeh Khajavi Fard^a, Zaynab Mokhtari^{a,b}

^a Department of Chemistry, Faculty of Nano and Bio Science and Technology, Persian Gulf University, Bushehr 75169, Iran

^b Department of Chemical Industry, Technical and Vocational University (TVU), Bushehr, Iran

ARTICLE INFO

Article history:

Received 28 September 2021

Revised 2 November 2021

Accepted 7 November 2021

Available online xxx

Keywords:

Ephedrine
Human serum albumin
Spectroscopy
Electrochemistry
Molecular docking

ABSTRACT

The aim of this study was to explore the efficiency of ephedrine binding to human serum albumin (HSA) as a protein model using spectroscopic, electrochemical, and molecular docking methods. A reduction in UV absorbance at 280 nm of HSA was attributed to the interaction between ephedrine and HSA. The apparent binding constant (K_{app}) values at different temperatures were about 10^4 M^{-1} , which showed high affinity of ephedrine for HSA. The calculated negative enthalpy change (ΔH) and entropy change (ΔS) values suggested that the binding process was mainly driven by van der Waals force and hydrogen bonds. The negative value of free energy change (ΔG) indicated that the interaction process was spontaneous. The results of cyclic voltammetry (CV) further confirmed the high affinity of ephedrine for HSA with an association constant of $2.73 \pm 0.17 \times 10^4 \text{ M}^{-1}$ at room temperature. Furthermore, molecular docking results revealed that ephedrine bound to site I in subdomain IIA via 2 hydrogen bonds with Phenylalanine 211 (Phe211) and Alanine 215 (Ala215) of HSA, and that Arginine 218 (Arg 218), Lysine 199 (Lys 199), and Serine 202 (Ser202) residues became involved in electrostatic interactions with ephedrine. Also, Leucine 198 (Leu198), Phe211, Tryptophan 214 (Trp214), Leu238, and Histidine 242 (His242) residues were responsible for the stability of the complex via hydrophobic interactions. Attenuated total reflection-Fourier transform infrared (ATR-FTIR) spectroscopy was used to investigate the conformational changes of HSA during the interaction of ephedrine and HSA.

© 2021 Elsevier B.V. All rights reserved.

1. Introduction

Ephedrine is an active medicinal constituent of the Ephedra plant (Scheme 1). It has been used widely for the treatment of rhinitis, bronchial asthma, and as a central nervous system stimulant [1–2]. Ephedrine has shown adverse reactions such as insomnia, nervousness, headache, tremor, hypertension, arrhythmias, heart attack, and even death [3].

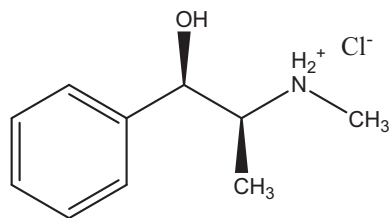
The interactions between transport proteins in plasma and drugs are very important in the pharmacokinetics and pharmacodynamics of drugs [4]. The binding of most of the drugs to plasma proteins is reversible, so the bound and free drug molecules are in dynamic equilibrium [5]. Drug-protein interaction needs to be carefully investigated and understood since it has a great influence on drug metabolism, circulation and free concentration. [6]. Today, with the development of novel drug delivery systems, the

importance of studying the interaction of drugs and proteins has increased and various studies have been conducted in this field [7–11].

In this research, we used human serum albumin (HSA) to investigate ephedrine-protein interaction. HSA is usually employed as a model protein because of its abundance in the circulatory system and its important role in the transport of many drugs [12]. HSA is a heart-shaped molecule and single-chain protein containing 585 amino acids. It is comprised of three homologous domains (I–III), and every domain is divided into two subdomains, A and B. Subdomains IIA and IIIA, which are situated in hydrophobic cavities, are known as major regions for drug binding sites. Sometimes, subdomain IB, is regarded as the binding site for drug molecules [5]. In general, more than 90 % of drug molecules are bound to HSA with high affinity. Serum albumin has an essential role in the maintenance of osmotic pressure and stabilization of the blood pH. Considering the correlation of protein structures and functions, binding of drugs causes a change in the conformational structure of proteins and affect their function [13]. In other

* Corresponding author.

E-mail address: shashemnia@pgu.ac.ir (S. Hashemnia).



Scheme 1. The chemical structure of ephedrine hydrochloride.

words, an understanding of the non-covalent binding interactions of drugs with HSA is of great interest and can provide insights into drug therapy and design [12,14–18].

In order to gain a more comprehensive insight into the pharmacological behaviors of ephedrine, it is very important to identify the interactions of ephedrine with HSA. Notwithstanding the common uses of ephedrine, there are very few reports about the interactions of ephedrine with HSA and the influences of this drug on protein structures [19–24]. To the best of our knowledge, there is no comprehensive report that uses electrochemical and molecular docking techniques along with a spectroscopic method to determine the affinity of the ephedrine towards serum albumin.

Therefore, in this research, we aimed to investigate the interaction between ephedrine and HSA under physiological pH conditions (pH 7.4) using spectroscopic and electrochemical techniques along with computational approaches [6–7]. For this purpose, the interaction was investigated through UV–Vis spectroscopy and cyclic voltammetry (CV). Some thermodynamic parameters, such as binding constants, ΔH , ΔG , and ΔS were also calculated. In addition, the conformational changes of HSA induced by ephedrine were examined through ATR-FTIR spectroscopy. The molecular docking data were confirmed by experimental results to obtain a better understanding of the mechanism involved in the interaction.

2. Materials and methods

2.1. Apparatus

The absorption spectra were recorded on an Analytic Jena, (SPECORD 250, Germany) UV–Vis spectrophotometer. Cyclic voltammetric measurements were performed with a Metrohm 797 VA Computrac (Switzerland) with a conventional three-electrode electrochemical system, including a glassy carbon electrode, an Ag/AgCl electrode, and a platinum electrode as the working, reference, and counter electrodes, respectively. Electrochemical impedance spectroscopy (EIS) measurements were carried out using a Zahner Zennium potentiostat/galvanostat (Germany). ATR-FTIR spectra were recorded at room temperature on a Jasco 4100 spectrometer (Jasco International, Tokyo, Japan).

2.2. Materials

Ephedrine hydrochloride (purity 99%) and human serum albumin (HSA) lyophilized powder, $\geq 97\%$ (agarose gel electrophoresis) were purchased from Sigma Aldrich (USA). Disodium hydrogen phosphate (Na_2HPO_4 , anhydrous $\geq 99.0\%$, MW: 141.96 g/mol), sodium dihydrogen phosphate dehydrate (NaH_2PO_4 , for analysis, MW: 156.006 g/mol), sodium chloride (NaCl, for analysis EMSURE, MW: 58.48 g/mol), potassium ferricyanide ($\text{K}_3[\text{Fe}(\text{CN})_6]$, for analysis EMSURE, MW: 329.24 g/mol), potassium ferrocyanide ($\text{K}_4[\text{Fe}(\text{CN})_6] \cdot 3\text{H}_2\text{O}$, for analysis EMSURE, MW: 422.39 g/mol) and Phosphoric acid (85%, for analysis EMSURE, MW: 98.00 g/mol) were obtained from Merck (Germany). All measurements were carried

out in a physiological aqueous solution of 0.1 M phosphate buffer with a pH of 7.4. The 0.1 M phosphate buffer (pH 7.4) was prepared by dissolving disodium hydrogen phosphate and sodium dihydrogen phosphate salts in distilled water, and the pH was adjusted by means of phosphoric acid and sodium hydroxide.

2.3. UV–Visible absorption studies of ephedrine–HSA complex

The UV–Visible absorption measurements of ephedrine and HSA in the absence and presence of different concentrations of ephedrine were carried out in the range of 250 to 350 nm wavelengths. HSA concentration was fixed at 2.0 μM , and the final concentration of ephedrine in the cell was varied from 0.0 to 150.0 μM . The HSA concentration was determined spectrophotometrically in the ultraviolet region (280 nm, molar absorbance coefficient (ϵ) = 36600 $\text{M}^{-1} \text{cm}^{-1}$) [25].

2.4. FT-IR spectra measurements

The FT-IR spectra of free HSA, ephedrine and ephedrine–HSA system in the phosphate buffer solution (PBS) (0.1 M, pH 7.4) were recorded in the range of 4000–400 cm^{-1} . All spectra were taken via the ATR method with a resolution of 4 cm^{-1} .

2.5. Cyclic voltammetry measurements

The bare glassy carbon electrode (GCE) was polished with 0.06 mm Al_2O_3 powder and cleaned ultrasonically in acetone and ultrapure water. Cyclic voltammograms of a PBS (pH 7.4, 0.1 M) containing NaCl (0.3 M) and $\text{K}_3\text{Fe}(\text{CN})_6/\text{K}_4\text{Fe}(\text{CN})_6$ (0.01 M) in the presence of HSA (2.0 μM) and different concentrations of ephedrine (0.0–150.0 μM) were recorded at a scan rate of 100 mV s^{-1} , using the three-electrode system. For this purpose, different amounts of the ephedrine solution were added continuously to the system and stirred. Before each measurement, the system was at rest for 3 min. All experiments were repeated 3 times at 27 $^\circ\text{C}$.

2.6. Molecular docking study

The molecular docking study of the HSA–ephedrine complexation was accomplished with AutoDock 4.2 software. The three-dimensional crystal structure of HSA (PDB ID:1IU6) was obtained from the RCSB Protein Data Bank. The structure of ephedrine was optimized using HyperChem Professional, and the proper format was obtained using OpenBabel v2.3.1. Site I of HSA was identified as the best binding site using blind docking in the whole structure of HSA. Then, the grid box was generated with coordinates $x = -3.715$, $y = 0.573$, and $z = -23.056$ Å, with the sizes of 24, 30, 26 Å for the specific docking site, respectively.

3. Results and discussion

3.1. Absorption characteristic of HSA–ephedrine interaction

To investigate the molecular interaction between ephedrine and HSA, the absorption spectra of the protein were recorded in the absence and presence of ephedrine. Fig. 1 shows the absorption spectra of HSA in the presence of increasing concentration of ephedrine at different temperatures. As seen, the absorption intensity at 280 nm decreases continuously as the ephedrine concentration is increased. The decrease in the absorption intensity may be attributed to the interaction of HSA and ephedrine. Therefore, the values of the binding constant for HSA interaction with ephedrine at different temperatures were estimated according to the absorption

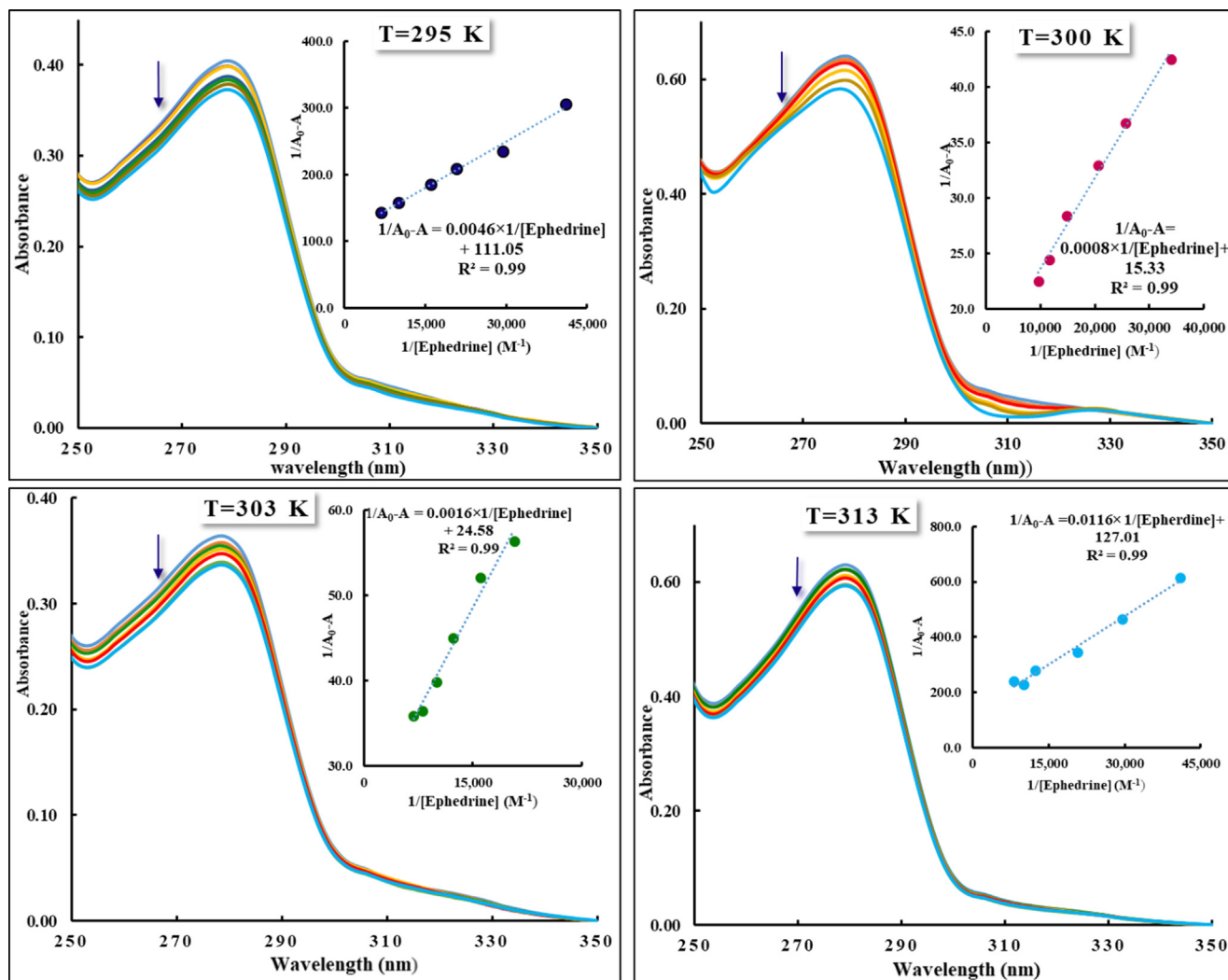


Fig. 1. The absorption spectra of HSA (2.0 μM) in the presence of increasing ephedrine concentration (0.0–150.0 μM) at different temperatures. The inset shows the plot of $1/A_0 - A$ versus $1/[ephe-drine]$.

Table 1

Thermodynamic parameters of the interaction of HSA with ephedrine at different temperatures.

Temperature (K)	K_{app}	ΔH (KJ/mol)	ΔS (J/mol)	ΔG (KJ/mol)
295	2.4×10^4	33.8	-30.7	-24.7
300	1.9×10^4			-24.6
303	1.4×10^4			-24.5
313	1.1×10^4			-24.2

data (inset of Fig. 1) by making use of the Benesi-Hildebrand equation. (Eq. (1)) [26].

$$\frac{1}{A_0 - A} = \frac{1}{A_0 - A_i} + \frac{1}{(A_0 - A_i) \times K_{app}} \times \frac{1}{[ephe-drine]} \quad (1)$$

where, A_0 is the absorbance of HSA at 280 nm in the absence of ephedrine, A is the absorbance of HSA at different concentrations of ephedrine, A_i is the absorbance of the protein at the infinite concentration of ephedrine, and K_{app} is the apparent binding constant. As seen in the inset of Fig. 1, the plot of $1/A_0 - A$ vs $1/[ephe-drine]$ is linear, and K_{app} can be estimated from the ratio of the intercept to the slope. Table 1 shows the K_{app} obtained at different temperatures.

Thermodynamic parameters, including enthalpy change (ΔH), entropy change (ΔS), and free energy change (ΔG) can be determined using the Van't Hoff equation (Eq. (2)) and Gibbs free energy equation (Eq. (3)), respectively. In general, ΔG reflects the possibility of reaction, whereas the quantities of ΔH and ΔS are judged to describe the type of binding forces [27–29]. Based on Eq. (2), ΔH and ΔS are calculated from the plot of $\ln K_{app}$ versus $1/T$ (Fig. S1), where K is the apparent binding constant at the corresponding temperature T , and R is the gas constant. Also, the Gibbs free energy was estimated by Eq. (3). The values of the thermodynamic parameters are presented in Table 1. As seen, in all cases, ΔG , ΔH , and ΔS are negative. The negative ΔH and ΔS values of the interaction between ephedrine and HSA suggest that the binding process is mainly driven by the van der Waals force and

hydrogen bonds. The negative value of ΔG indicates that the interaction process is spontaneous [30–31].

$$\ln K_{app} = \frac{-\Delta H}{R} \times \frac{1}{T} + \frac{\Delta S}{R} \quad (2)$$

$$\Delta G = \Delta H - T\Delta S \quad (3)$$

3.2. Cyclic voltammetry investigations

To further confirm the results obtained using the UV-Visible spectroscopic method, we used cyclic voltammetry as an effective method to investigate the interaction between HSA and ephedrine under the physiological pH conditions [32–34]. For this purpose, the electrochemical behavior of $K_3Fe(CN)_6/K_4Fe(CN)_6$ probe at the GCE surface was investigated in the presence of HSA and HSA-ephedrine at a scan rate of 0.1 Vs^{-1} (Fig. 2). As seen in Fig. 2, the $K_3Fe(CN)_6/K_4Fe(CN)_6$ redox couple shows a good electrochemical response with a pair of redox peaks. The redox couple represented a peak potential separation about 0.619 V and 0.624 V in the absence and presence of the ephedrine, respectively. However, in the presence of HSA, in addition to the increase in peak potential separation (1.052 V), the formal peak potential was negatively shifted and the redox peak current decreased. Furthermore, by the addition of ephedrine, in the presence of HSA, the redox peak currents were further decreased, and the separation of the redox peak potential increased to 1.082 V. These results suggested that the variations occurring on the electron transfer between the electrode surface and $K_3Fe(CN)_6/K_4Fe(CN)_6$ redox couple were related to the interactions between HSA and ephedrine. Therefore, this electrochemical system was subsequently used to investigate the interaction between ephedrine and HSA.

To investigate the electron transfer kinetics of $K_3Fe(CN)_6/K_4Fe(CN)_6$ probe at the GCE surface in the presence of HSA ($2.0 \mu\text{M}$) and ephedrine ($24.0 \mu\text{M}$), the corresponding cyclic voltammograms were recorded at different scan rates (Fig. 3(A-D)). The plot of \log

I_{pa} (anodic peak current) versus $\log v$ (scan rate) showed a linear relationship with a slope of less than 0.5 in each case, indicating that the redox reaction at the electrode surface was a diffusion-controlled process (inset (I) in Fig. 3(A-D)). The cyclic voltammetric method was subsequently used to investigate the interaction between ephedrine and HSA. As seen in Fig. 2, when the drug was added into the $K_3Fe(CN)_6/K_4Fe(CN)_6$ electrolyte solution, a small decrease in the redox peak currents was observed. However, in the presence of HSA, the decrease in the peak currents and the negative shift in the peak potentials were very significant (Fig. 2, curve c). The later decrease in the redox peak currents and the negative shift of the redox peak potentials after the addition of ephedrine in the presence of HSA (Fig. 2, curve d) might have resulted from the interaction between HSA and ephedrine that reduced the electron transfer rate constant of $K_3Fe(CN)_6/K_4Fe(CN)_6$ subsequently (Table 2). According to the diffusion-controlled process of $K_3Fe(CN)_6/K_4Fe(CN)_6$ at the electrode surface, the plot of anodic or cathodic peak potentials against $\ln v$ showed a good linear relationship (inset (II) in Fig. 3(A-D)).

In these circumstances, based on the slope and intercept of the plot (Fig. 4), the standard rate constant can be obtained from the following equations (Eqs. 4–7) [35].

$$E_{pa} = E^\circ + m \left[0.78 + \ln \left(\frac{D^{1/2}}{k'} \right) - 0.5 \ln m \right] + 0.5m \ln v \quad (4)$$

$$m = \frac{RT}{[(1-\alpha)nF]} \quad (5)$$

$$E_{pc} = E^\circ - m' \left[0.78 + \ln \left(\frac{D^{1/2}}{k'} \right) - 0.5 \ln m' \right] - 0.5m' \ln v \quad (6)$$

$$m' = \frac{RT}{[\alpha nF]} \quad (7)$$

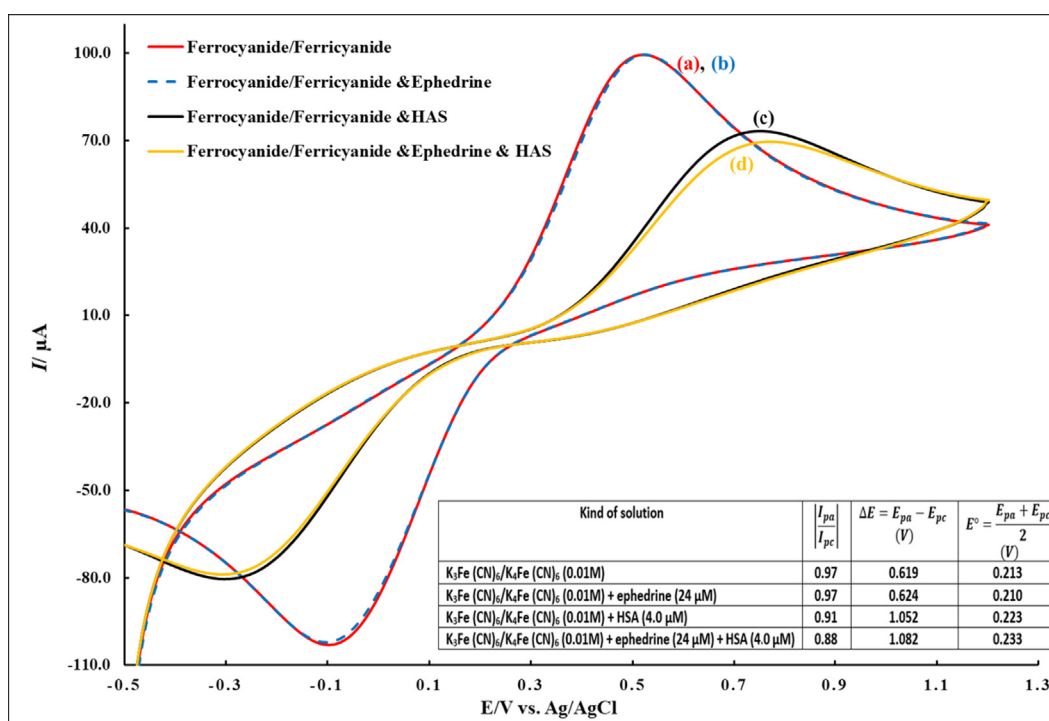


Fig. 2. The electrochemical behavior of $K_3Fe(CN)_6/K_4Fe(CN)_6$ probe in the (a) absence and (c) presence of HSA ($4.0 \mu\text{M}$) and in the presence of (b) ephedrine ($24 \mu\text{M}$) and (d) HSA-ephedrine at a scan rate of 0.1 Vs^{-1} . The inset shows the corresponding electrochemical parameters of each voltammogram.

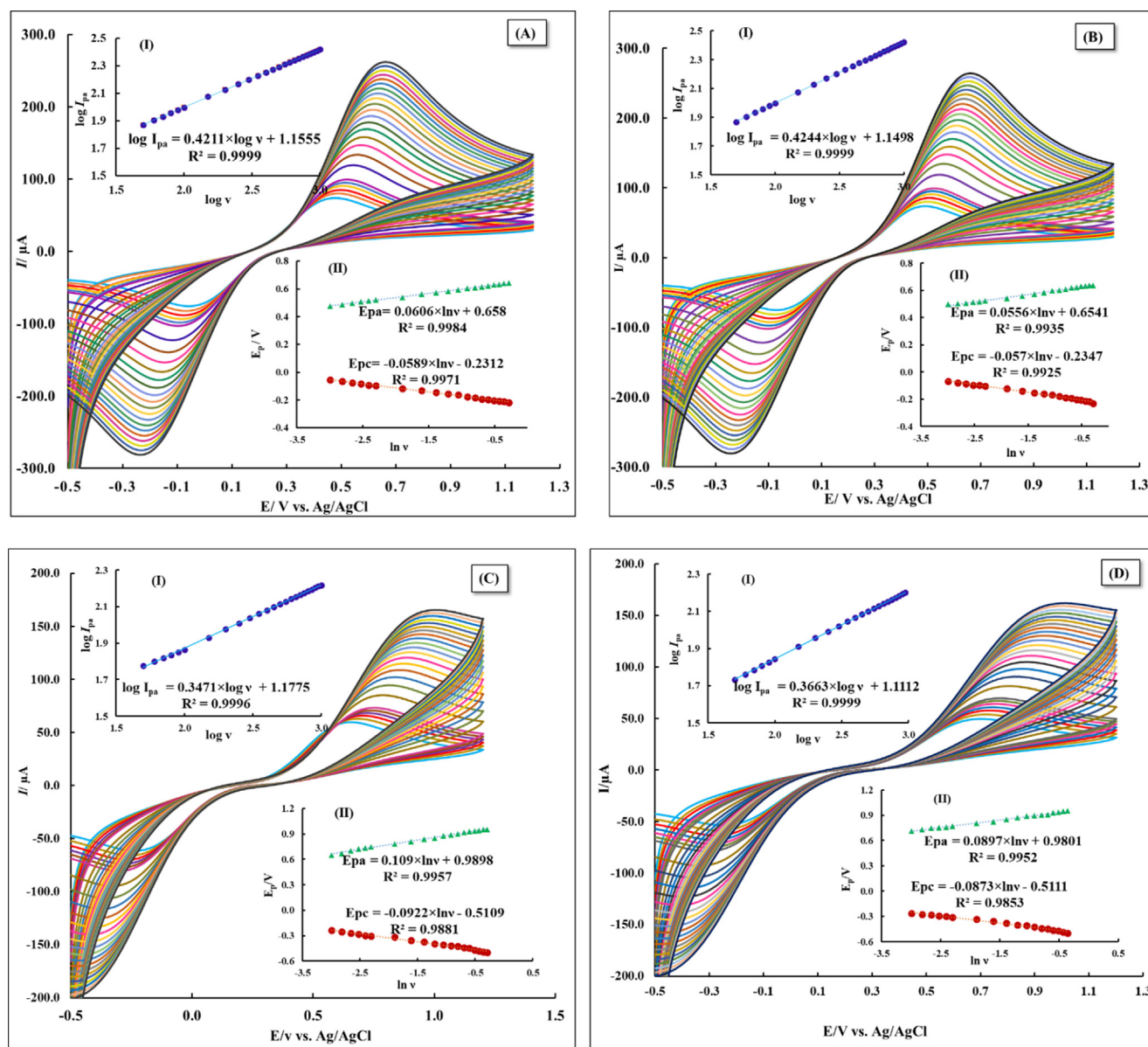


Fig. 3. The cyclic voltammograms of $K_3Fe(CN)_6/K_4Fe(CN)_6$ redox pair in solutions containing (A): $K_3Fe(CN)_6/K_4Fe(CN)_6$ (0.01 M), (B): $K_3Fe(CN)_6/K_4Fe(CN)_6$ (0.01 M) + ephedrine (24 μM), (C): $K_3Fe(CN)_6/K_4Fe(CN)_6$ (0.01 M) + HSA (2.0 μM), (D): $K_3Fe(CN)_6/K_4Fe(CN)_6$ (0.01 M) + ephedrine (24 μM) + HSA (2.0 μM) at different scan rates. Insets (I(A-D)) show the plot of $\log I_{pa}$ (anodic peak current) versus $\log v$ (scan rate). Insets (II(A-D)) show the plot of E_p versus $\ln v$.

Table 2

The kinetic parameters (α , the charge transfer coefficient, K° , and the electron transfer rate constant) obtained for $K_3Fe(CN)_6/K_4Fe(CN)_6$ redox couples in the absence and presence of ephedrine and HSA.

Kind of solution	E° (V)	α	K°
$K_3Fe(CN)_6/K_4Fe(CN)_6$ (0.01 M)	0.212	0.51	4.21×10^{-4}
$K_3Fe(CN)_6/K_4Fe(CN)_6$ (0.01 M) + ephedrine (24 μM)	0.211	0.49	3.50×10^{-4}
$K_3Fe(CN)_6/K_4Fe(CN)_6$ (0.01 M) + HSA (2.0 μM)	0.220	0.54	3.00×10^{-4}
$K_3Fe(CN)_6/K_4Fe(CN)_6$ (0.01 M) + ephedrine (24 μM) + HSA (2.0 μM)	0.231	0.51	2.00×10^{-4}

where E_{pa} (V) and E_{pc} (V) represent the anodic and cathodic peak potentials, respectively; v (Vs^{-1}) denotes the scan rate; α is the charge transfer coefficient; K° is the electron transfer rate constant; n is the electron transferred number; T is Kelvin temperature; F is the Faraday constant ($96480C mol^{-1}$); and R is a

universal gas constant ($8.314 J/mol^{-1} K^{-1}$). Using the plot of E_{pa} / E_{pc} versus $\ln v$ and equations (4)–(7), the charge transfer coefficient α and K° could be estimated. Table 2 shows the values of these parameters. As seen, the electron transfer rate constant (K°) is reduced in the presence of ephedrine and HSA, suggesting that

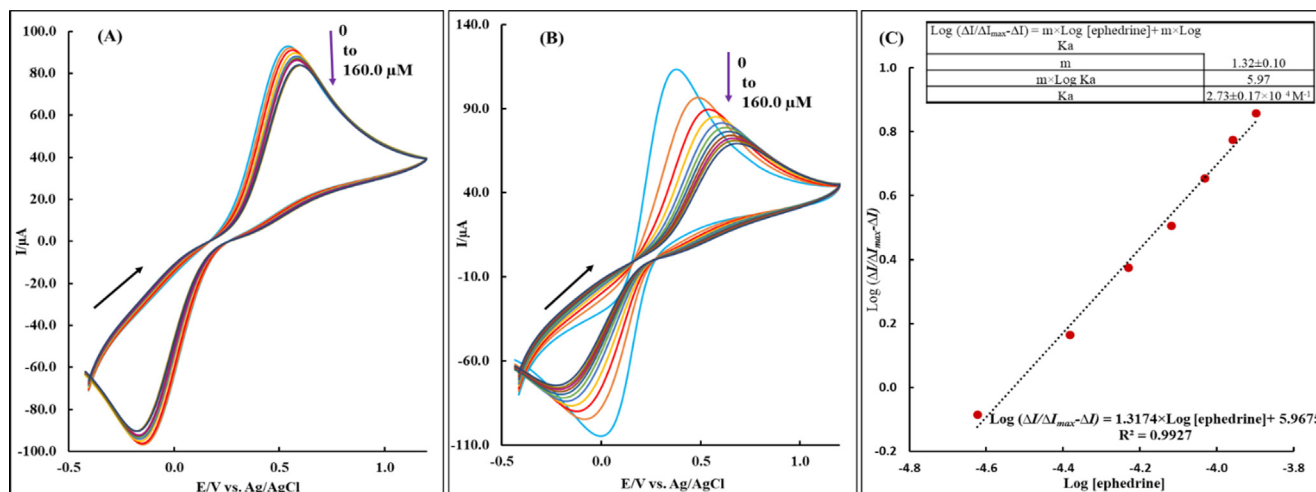
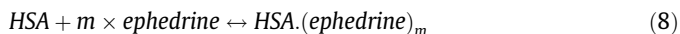


Fig. 4. The cyclic voltammograms of the electrolyte solution containing 0.01 M $K_3Fe(CN)_6/K_4Fe(CN)_6$; (A) in the absence and (B) presence of HSA (2.0 μM) with varying ephedrine concentrations (0.0–160.0 μM). (C) The plot of $\log(\Delta I/(\Delta I_{max} - \Delta I))$ versus $\log[\text{ephedrine}]$

the interaction between the drug and the protein may decrease the diffusion rate of the electroactive species ($K_3Fe(CN)_6/K_4Fe(CN)_6$ redox couples) towards the electrode surface.

If it is assumed that HSA and ephedrine produce a single complex ($HSA.(ephedrine)_m$), as shown in the following reaction (Eq. (8)) [36],



the decrease in the peak current intensity of cyclic voltammograms in the presence of different concentrations of ephedrine is proportional to the concentration of the $HSA.(ephedrine)_m$ complex. The fraction of HSA to which ephedrine is bound as $HSA.(ephedrine)_m$ in proportion to the total concentration of the protein in the supporting electrolyte $[HSA]_0 = [HSA.(ephedrine)_m]_{max}$ is defined as (Eq. (9)) [37]:

$$f = \frac{[HSA.(ephedrine)_m]}{[HSA.(ephedrine)_m]_{max}} = \frac{[ephedrine]^m}{[ephedrine]^m + K_d^m} \quad (9)$$

$$K_d^m = \frac{[ephedrine]^m(1-f)}{f} \quad (10)$$

where, $[HSA.(ephedrine)_m]_{max}$ is the maximum concentration of the complex, $[ephedrine]$ is the concentration of free ephedrine, K_d (Eq. (10)) is the dissociation equilibrium constant, and m is the Hill coefficient. Note that $K_d = [ephedrine]_{0.5}$, that is K_d is equal to the ephedrine concentration at half occupation, and the association constant K_a is the inverse of K_d . It is not advisable to use the overall constant $K=(K_a)^m$, which would have the physically meaningless dimension of M^{-m} . The interaction partners for ephedrine are the binding sites of HSA. From mass conservation, we get (Eqs. 11–13):

$$[HSA] = [HSA.ephedrine_m]_{max} - [HSA.ephedrine_m] \quad (11)$$

$$[ephedrine] - m[HSA.ephedrine_m] \quad (12)$$

$$[ephedrine] = [ephedrine]_0 - m[HSA.ephedrine_m] \quad (13)$$

Where, $[ephedrine]_0$ is the total concentration of ephedrine. In view of the decrease in the redox peak currents after the addition of ephedrine and Ilkovic equation (Eq. (14)) [38],

$$I = K \times [ephedrine] \quad (14)$$

where, K is a constant. In this way, the difference in currents (ΔI) is defined as (Eqs. 15–17):

$$\Delta I = K([ephedrine]_0 - [ephedrine]) \quad (15)$$

$$\Delta I = K \times m[HSA.ephedrine_m] \quad (16)$$

$$\Delta I_{max} = K \times m[HSA.ephedrine_m]_{max} \quad (17)$$

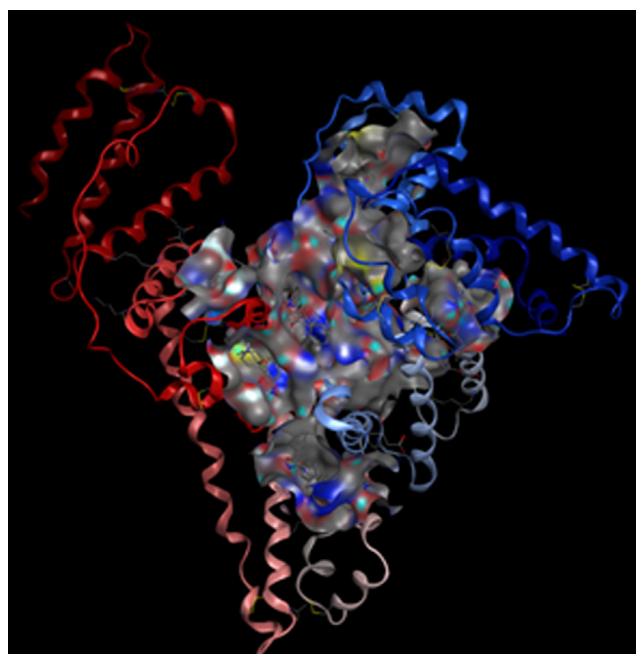


Fig. 5. Probable binding sites of ephedrine in the HSA complex.

Table 3

The values of the equivalent circuit parameters obtained using Zview software.

Kind of solution	Rs (Ω)	Rct (Ω)	W ₀ (Ω)
$K_3Fe(CN)_6/K_4Fe(CN)_6$ (0.01 M)	16.1	106.7	0.7
$K_3Fe(CN)_6/K_4Fe(CN)_6$ (0.01 M) + ephedrine (50 μM)	17.5	106.8	2.1
$K_3Fe(CN)_6/K_4Fe(CN)_6$ (0.01 M) + HSA (2.0 μM)	17.6	66.3	175.1
$K_3Fe(CN)_6/K_4Fe(CN)_6$ (0.01 M) + ephedrine (50.0 μM) + HSA (2.0 μM)	17.5	60.1	209.3

From equation (9), we obtain

$$\log \left[\frac{f}{1-f} \right] = m \log K_a + m \log [\text{ephedrine}] \quad (18)$$

Insertion of equations (16) and (17) into equation (18) yields (Eq. (19)):

$$\log \left[\frac{\Delta I}{\Delta I_{\max} - \Delta I} \right] = m \log K_a + m \log [\text{ephedrine}] \quad (19)$$

To determine the association constant of the $\text{HSA} \cdot (\text{ephedrine})_m$ complex, the cyclic voltammograms of the electrolyte solution containing 0.01 M $\text{K}_3\text{Fe}(\text{CN})_6/\text{K}_4\text{Fe}(\text{CN})_6$ in the absence and presence of HSA (2.0 μM) with varying ephedrine concentrations (0.0–160.0 μM) were recorded (Fig. 4A and 4B, respectively). As seen in the absence of HSA, the I_{pa} and I_{pc} change slightly with increasing the ephedrine concentration, whereas in the presence of the protein, along with a shift in the formal potential (from 0.210 V to 0.233 V), the decrease in the I_{pa} and I_{pc} is more considerable. Therefore, all of the anodic peak currents were corrected as $I_{pa} = I_{pa \text{ in the absence of HSA}} - I_{pa \text{ in the presence of HSA}}$. In the next step, considering Eq. 19, the graph of $\log[\Delta I/(\Delta I_{\max} - \Delta I)]$ as a function of $\log[\text{ephedrine}]$ (M) was plotted (Fig. 4C). According to the linear equation and the slope of the curve in Fig. 4C, the value of the association constant K_a was $2.73 \pm 0.17 \times 10^4 \text{ M}^{-1}$, which was a little higher than the value of the binding constant obtained by the UV-Visible spectroscopic method.

3.3. Electrochemical impedance spectroscopy

To further investigate the ephedrine-HSA interaction, electrochemical impedance spectroscopy (EIS) was carried out in the frequency range of 100 kHz and 0.05 Hz with an AC perturbation of 5 mV. All measurements were performed in phosphate buffer solution (pH 7.4, 0.1 M) containing NaCl (0.3 M), $\text{K}_3\text{Fe}(\text{CN})_6/\text{K}_4\text{Fe}(\text{CN})_6$ (0.01 M). Fig. S2 shows the Nyquist plots of the impedance spectra of $\text{K}_3\text{Fe}(\text{CN})_6/\text{K}_4\text{Fe}(\text{CN})_6$ redox pair in the absence and presence of HSA and ephedrine, which were obtained at 0.4 V versus Ag/AgCl. The value of the potential was chosen in accordance with the shape of the voltammograms. Nyquist plots can be described as semicircles in high frequency regions, followed by a linear tail with a slope of near unity at a very low frequency. The linear tail has been attributed to the diffusion of $\text{K}_3\text{Fe}(\text{CN})_6/\text{K}_4\text{Fe}(\text{CN})_6$ as the redox

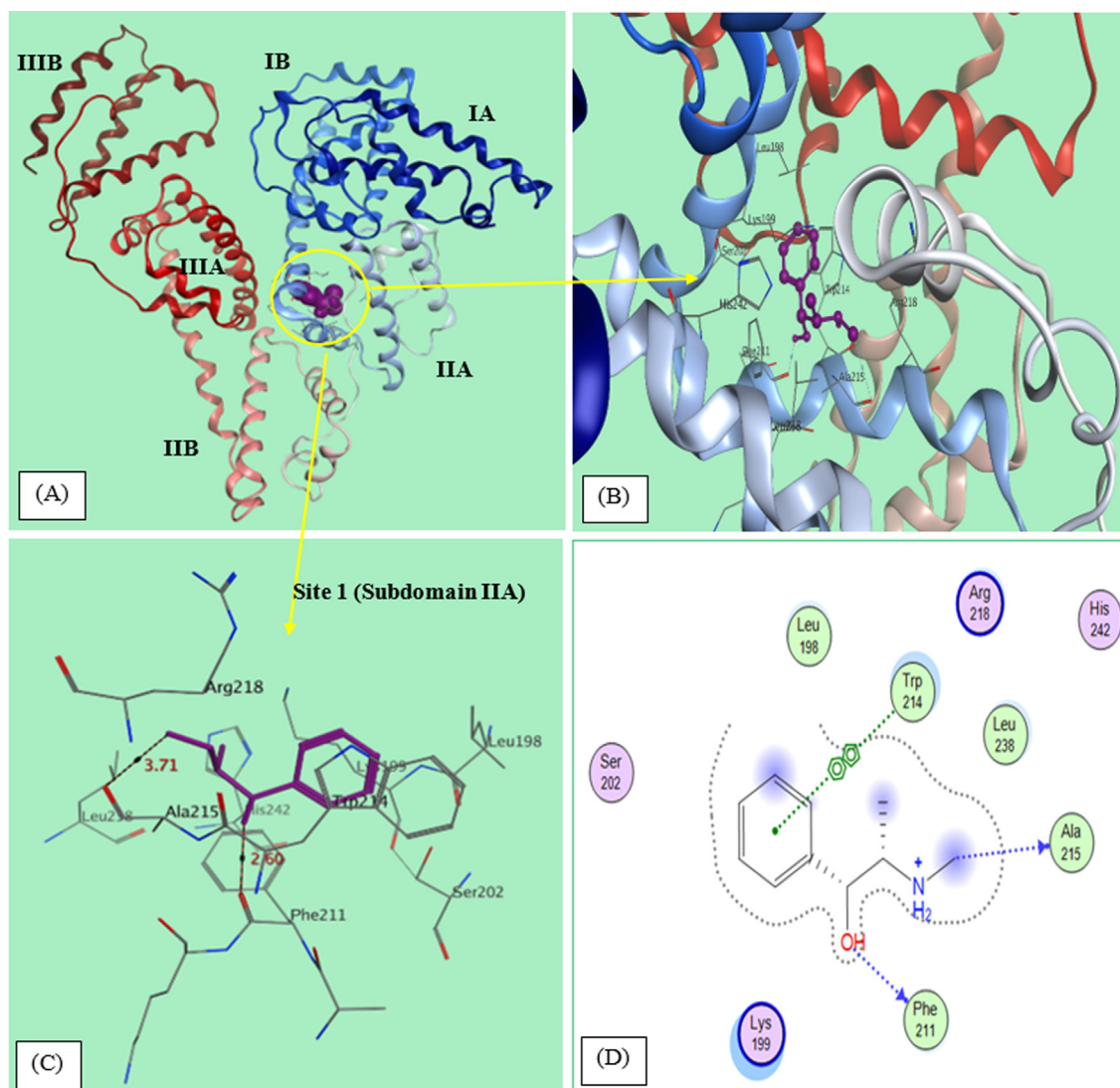


Fig. 6. (A) 3D view of the molecular docking state of ephedrine with HSA protein (PDB ID: 1Lu6). (B) 3D image of ephedrine interactions with the residues of site 1 in HSA (HSA is shown using ribbons and ephedrine as sticks). (C) Ephedrine surrounded by the hydrophobic binding cavity of HSA. (D) 2D diagram of ephedrine and HSA interactions. (The arrow tips represent the H-bond donors).

probe (Warburg Impedance, W_0) [39]. The equivalent circuit for fitting the EIS data contains the internal resistance (R_s , related to the electrolyte or sample solution resistance), the charge transfer resistance (R_{ct}), the double layer capacitance (C_{dl}), and the Warburg impedance (W_0 , related to linear tail), which is shown in the inset of Fig. S2. The parameters were fitted by Zview, and the values of each component are shown in Table 3. As seen, the values of the resistance of the electrolyte solution (R_s) and the electrode charge transfer remain constant for solutions containing ephedrine, HSA, and HSA-ephedrine. However, the value of Warburg impedance (W_0) for the solution containing $K_3Fe(CN)_6/K_4Fe(CN)_6$ only is 0.7Ω and is increased to 2.1, 175.5 and 209.3Ω for the solutions containing the redox probe in the presence of HSA ($2.0 \mu M$), ephedrine ($50.0 \mu M$), and HSA-ephedrine, respectively, which proves that the interaction between ephedrine and the protein affects the diffusion of the redox probe towards the electrode surface.

3.4. Molecular docking study

Molecular docking was also used to demonstrate probable intermolecular interactions between ephedrine and HSA and the participation of possible thermodynamic interactions throughout the complexation. For this purpose, HSA was considered as a receptor and docked with the ephedrine molecule as a ligand. The blind docking analysis of the whole surface of HSA revealed that the main binding sites for ephedrine molecules were located in the sub-domains (IA, IB and IIA) (Fig. 5).

The best conformation was selected for further study owing to its lowest binding energy (-23.82 kJ/mol), which was in agreement with the binding energy found spectrophotometrically (Table 1). Fig. 6A shows the stereo view of the docking state of ephedrine with HSA, which demonstrates that site I (in subdomain IIA) of HSA was favorable for ephedrine-HSA association. Fig. 6 (B-

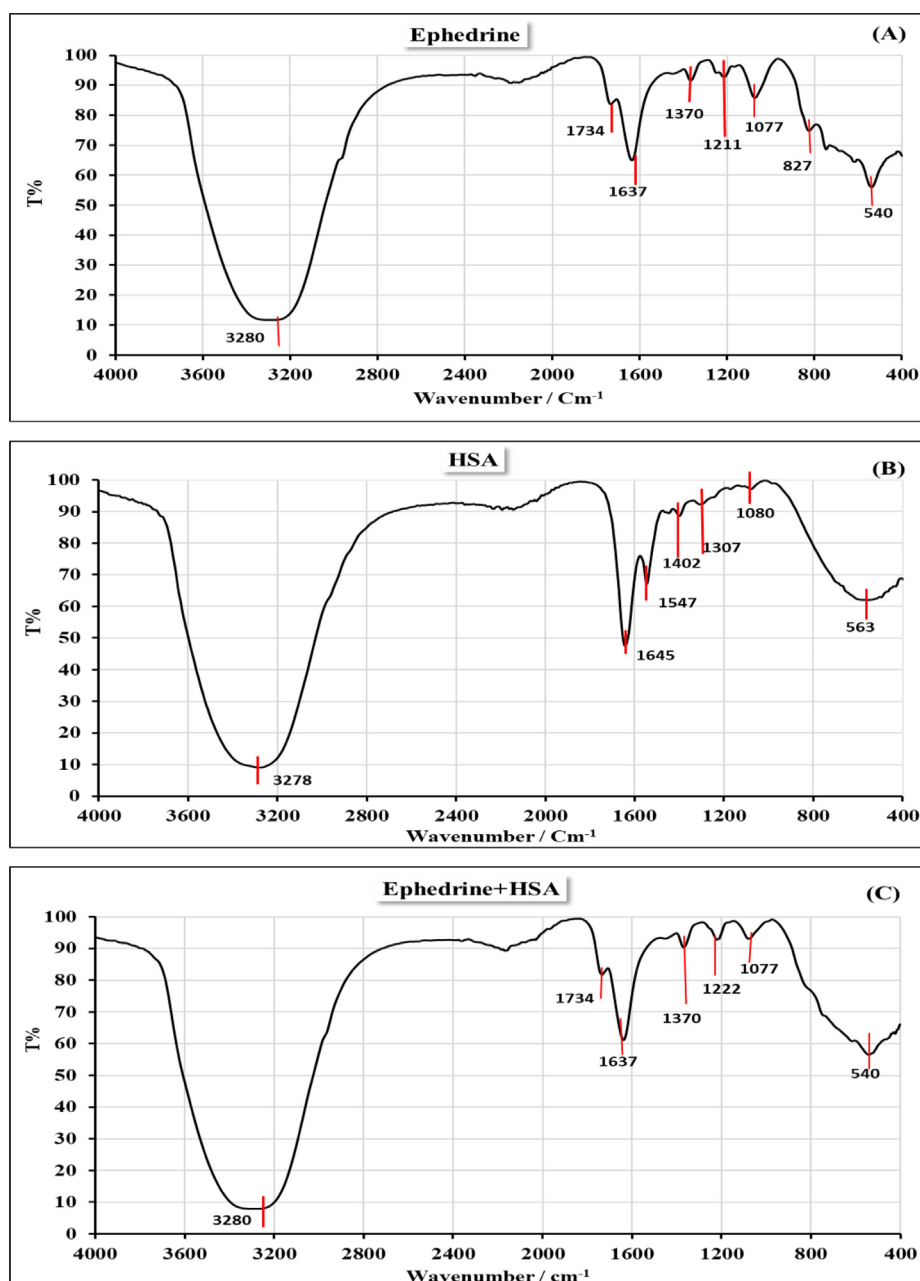


Fig. 7. ATR FT-IR spectra of (A) HSA, (B) ephedrine and (C) ephedrine –HSA system in PBS (0.1 M, pH 7.4). All the spectra were recorded in the $4000\text{--}400 \text{ cm}^{-1}$ regions.

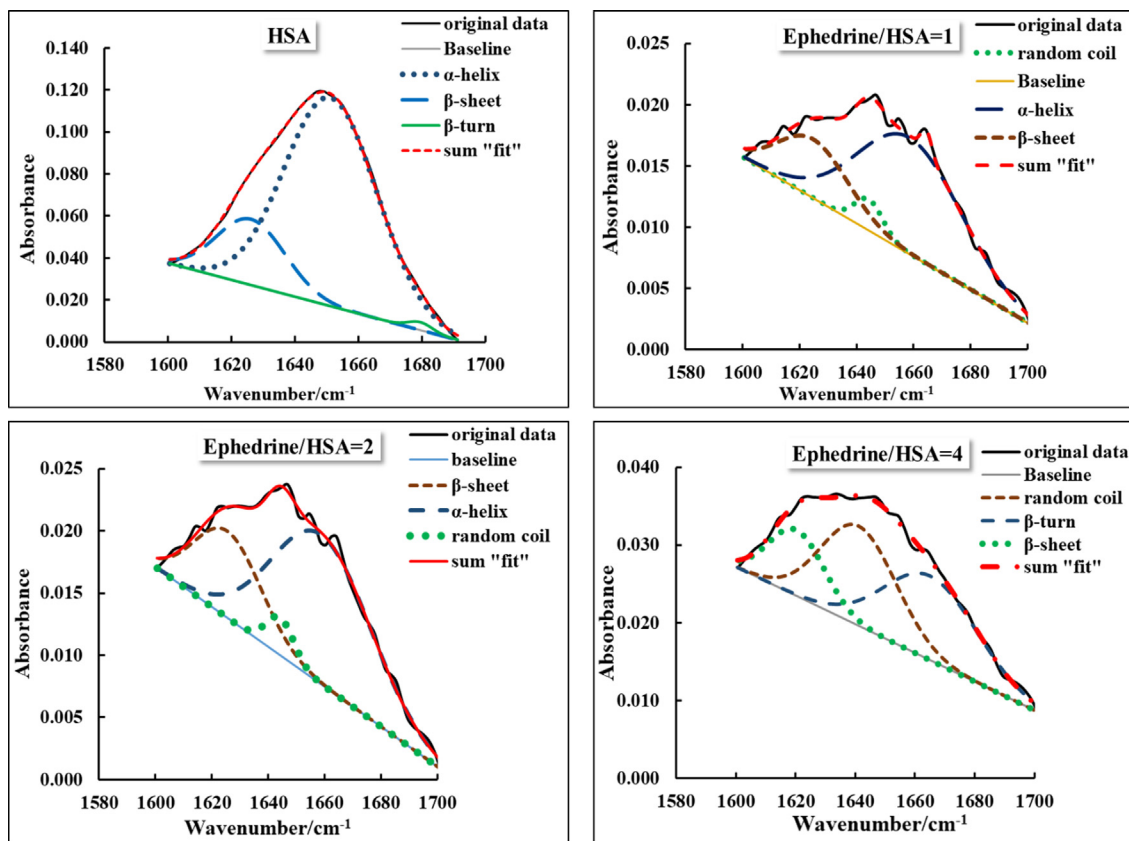


Fig. 8. Gaussian curve fitting of the deconvoluted spectra of HSA and ephedrine-HSA with different ratios of ephedrine/HSA in the amide I region.

D) shows that ephedrine can form two hydrogen bonds between phe211 and Ala215 in the interaction cavity close to Trp 214, with bond lengths of about 2.6 Å and 3.71 Å, respectively [40]. Furthermore, a number of charged and polar residues, such as Arg 218, Lys 199, and Ser202, were involved in HSA and ephedrine association via electrostatic interactions. Also, Leu198, Phe211, Trp214, Leu238 and His242 residues were responsible for the ephedrine and HSA complex stability via hydrophobic interactions (Fig. S3) [41–43]. It is noteworthy that decrease in the UV absorbance at

278 nm may be assigned to the ephedrine hydrophobic interactions with the aromatic amino acid residue Trp214 [43].

3.5. ATR-FTIR experiment

ATR-FTIR spectroscopy was performed in the range of 4000 to 400 cm^{-1} to further characterize the protein and ephedrine interaction. As seen in Fig. 7A, ephedrine hydrochloride shows a broad band at 3280 cm^{-1} , related to the stretching vibration of O-H group. The peaks observed in the range of 1370–1077 cm^{-1} are attributed to the vibrations of the aromatic ring. The peaks below 1000 cm^{-1} (827 and 540 cm^{-1}) indicate C-H out of plane deformation, that is, mono-substituted benzene. Furthermore, the peaks at 1637 cm^{-1} and 1734 cm^{-1} are attributed to the bending vibrations of the hydrogen bond and the protonated N-H group [44].

The ATR-FTIR spectrum of HSA in the aqueous solution was also recorded in the spectral region of 4000 to 400 cm^{-1} (Fig. 7B). The spectrum showed several amide bands, including the amide I region (1600–1700 cm^{-1}) with a maximum at 1645 cm^{-1} , which corresponded to C=O stretching vibration, and amide II region (1500–1550 cm^{-1}) with a maximum at 1547 cm^{-1} , which corresponded to the C-N stretching vibration coupled to the N-H bend-

Table 4

Vibrational frequency range (cm^{-1}) associated with secondary structure of HSA in the amide I region used for curve fitting in this work and the literature.

Secondary structure assignment	Vibrational frequency range (cm^{-1})	
	References [45–46]	Peak centers found in this work
α -helix	1650–1660	1651, 1658
β -sheet	1620–1639, 1689–1695	1620–1625
β -turn	1660–1689	1665, 1679
Random Coil	1642–1648	1641, 1644

Table 5

Percentages of secondary structural contributions in the ATR- FTIR spectra of HSA and ephedrine-HSA.

Samples	α -helix, % (wavenumber, cm^{-1})	β -sheet, % (wavenumber, cm^{-1})	β -turn, % (wavenumber, cm^{-1})	Random Coil, % (wavenumber, cm^{-1})	Chi-square	R ²
HSA	80.6 (1651)	18.6 (1621)	0.8 (1679)	–	6.6×10^{-7}	0.999
Ephedrine/HSA = 1	70.1 (1658)	23.4 (1624)	–	6.5 (1644)	1.5×10^{-7}	0.991
Ephedrine/HSA = 2	68.5 (1658)	26.7 (1625)	–	4.8 (1644)	2.1×10^{-7}	0.991
Ephedrine/HSA = 4	–	19.3 (1620)	40.7 (1665)	40.0 (1641)	2.4×10^{-7}	0.994

Table 6
Comparison of the results reported in various papers on ephedrine and albumin (BSA or HSA) interactions.

The aim of study	Binding constant /M ⁻¹	Reported Driving forces	Spectroscopic techniques	Electrochemical techniques	Computational modeling	Other techniques	Ref
Investigation of the interaction between ephedrine and pseudoephedrine with HSA	2.02×10^4	Hydrogen bond and Vander Waals	Uv spectroscopy, fluorescence and synchronous fluorescence	-	-	-	[19]
Investigation of the interaction between ephedrine, caffeine and acetaminophen with BSA	3.38×10^4	-	-	-	-	Capillary electrophoresis with the partial filling technique	[20]
BSA as buffer additive for chiral separation of Ephedrine and pseudoephedrin	-	-	-	-	-	Capillary electrophoresis	[23]
Determination of ephedrine in human urine, and a study of its interactions with BSA, cytochrome C, myoglobin	1.55×10^4	-	-	Electrochemiluminescence	-	Capillary electrophoresis coupled with end-column electrochemiluminescence	[47]
Determination of plasma protein binding for sympathomimetic drugs	From Scatchard plot 6.16×10^{-3} 1.12×10^{-3} From Klotz plot 1.04×10^{-2} 1.28×10^{-3}	-	-	-	-	Ultrafiltration (continuous and discontinuous)	[24]
Comprehensive insight into the interactions of ephedrine and HSA	From spectroscopic 2.40×10^4 from electrochemical 2.73×10^4	van der Waals force and hydrogen bond	Uv spectroscopy, FTIR spectroscopy	cyclic voltammetry (CV) Electrochemical impedance spectroscopy (EIS)	Molecular docking	-	This work

ing vibration of the amide group. These vibrations are related to the secondary structure of the protein, and the amide I band can be used to investigate the secondary structure and conformational changes of the protein [34]. As seen in Fig. 7C, the amide I and II bands disappeared in the presence of ephedrine. To study the effect of the drug on the amide I band more precisely, the spectrum software of the FTIR device was used to convert the spectra from transmittance to absorbance and to perform baseline correction. Background subtraction for all solutions obtained in PBS was done using the spectrum of the buffer. Then, the amide I region of the obtained spectra was deconvoluted using Origin Pro 2021. The peak analyzer tool of this software was used to identify hidden peaks in the deconvoluted amide I region, assuming a Gaussian curve fit. In the deconvolution process, the baseline was fitted as a straight line between 1700 and 1600 cm⁻¹, and the second derivative spectrum was determined to find the initial peak positions for peak fitting. Then, according to the positions suggested by the second derivative spectrum, the Gaussian peaks were added to the amide I band. This procedure was applied for the aqueous spectra of HSA and ephedrine-HSA with different ratios of ephedrine/HSA, and the correlation coefficients (R²) for the deconvolution fits were ≥ 0.99 (Fig. 8). The observable related secondary structures (including α -helix, β -sheet, β -turn, and random coil) in the amide I region of FTIR spectra which were obtained in this work and the literature are summarized in Table 4. As reported in Table 5, the secondary structure of the protein changed considerably with increase in the concentration of ephedrine. There is a loss of the α -helix structure, along with a gain of β -sheet, β -turn and random coil structures by increasing the ephedrine concentration.

4. Conclusion

The interaction between ephedrine and HSA was investigated by ultraviolet and ATR-FTIR spectroscopy, cyclic voltammetry, electrochemical impedance spectroscopy, and molecular docking study. Results show that ephedrine interacted with HSA in physiological conditions and affected protein conformation at tertiary and second structural levels. The negative value of ΔG indicated the spontaneity of the ephedrine-HSA complex formation. The negative ΔH and ΔS values of the complex suggest that the binding process was mainly driven by the van der Waals force and hydrogen bonds and that the complex formation was an exothermic process.

The interaction of HSA with ephedrine was also proved by both cyclic voltammetry and electrochemical impedance spectroscopy. The variation of electrochemical parameters for both CV and EIS show that the association constant of the ephedrine-HSA complex was in good agreement with the value obtained by the spectroscopy method. The results show that the electrochemical method is potentially useful for investigating interaction between drugs and proteins and can be utilized in pharmaceutical and biochemistry fields. The affinity of ephedrine towards albumin HSA has been reported before (Table 6), but compared with the published articles, this work has drawn on more approaches (spectroscopic, electrochemical and molecular docking) to investigate the affinity of ephedrine towards albumin. In view of the consistency of the results obtained by using different methods, this work can prove particularly helpful.

Declaration of Competing Interest

The authors declare that they have no known competing financial interests or personal relationships that could have appeared to influence the work reported in this paper.

Acknowledgments

We gratefully acknowledge the financial support of the Research Council of Persian Gulf University.

Appendix A. Supplementary material

Supplementary data to this article can be found online at <https://doi.org/10.1016/j.molliq.2021.118058>.

References

- R.P. Limberger, A.L.B. Jacques, G.C. Schmitt, M.D. Arbo, Pharmacological effects of ephedrine, *J. Nat. Prod.* 38 (2013) 1217–1237, https://doi.org/10.1007/978-3-642-22144-6_41.
- L.C. Sander, K.E. Sharpless, M.B. Satterfield, T. Ihara, K.W. Phinney, J.H. Yen, S.A. Wise, M.L. Gay, J.W. Lam, M. McCooney, G. Gardner, C. Fraser, R. Sturgeon, M. Roman, Determination of ephedrine alkaloids in dietary supplement standard reference materials, *Anal. Chem.* 77 (10) (2005) 3101–3112, <https://doi.org/10.1021/ac0484530>.
- J. Hou, J. Zheng, S.A.A. Rizvi, S.A. Shamsi, Simultaneous chiral separation and determination of ephedrine alkaloids by MEKC-ESI-MS using polymeric surfactant I: Method development, *Electrophoresis* 28 (9) (2007) 1352–1363, <https://doi.org/10.1002/elps.200600415>.
- N. Maurya, J.K. Maurya, U.K. Singh, R. Dohare, M.d. Zafaryab, M. Moshahid Alam Rizvi, M. Kumari, R. Patel, In vitro cytotoxicity and interaction of nescapine with human serum albumin: effect on structure and esterase activity of HSA, *Mol. Pharm.* 16 (3) (2019) 952–966, <https://doi.org/10.1021/acs.molpharmaceut.8b00864>.
- S. Panja, D.K. Khatua, M. Halder, Simultaneous binding of folic acid and methotrexate to human serum albumin: insights into the structural changes of protein and the location and competitive displacement of drugs, *ACS omega* 3 (1) (2018) 246–253, <https://doi.org/10.1021/acsomega.7b01437>.
- M.A. Rub, J.M. Khan, N. Azum, A.M. Asiri, Influence of antidepressant clomipramine hydrochloride drug on human serum albumin: spectroscopic study, *J. Mol. Liquids* 241 (2017) 91–98, <https://doi.org/10.1016/j.molliq.2017.05.143>.
- F. Khan, D. Kumar, N. Azum, M.A. Rub, A.M. Asiri, Effect of salt and urea on complexation behavior of pharmaceutical excipient gelatin with phenothiazine drug promazine hydrochloride, *J. Mol. Liquids* 208 (2015) 84–91, <https://doi.org/10.1016/j.molliq.2015.04.024>.
- J. Abedin, S. Mahbub, M.M. Rahman, A. Hoque, D. Kumar, J.M. Khan, A.M. El-Sherbeeny, Interaction of tetradecyltrimethylammonium bromide with bovine serum albumin in different compositions: effect of temperatures and electrolytes/urea, *Chin. J. Chem. Eng.* 29 (2021) 279–287, <https://doi.org/10.1016/j.cjche.2020.07.062>.
- N.J. Mukta, S. Mahbub, M.J. Abedin, M.E. Hossain, D. Kumar, M.A. Hoque, M.A. Khan, M.T. Rehman, N. Azum, M. Akram, H.M. Marwani, Effect of Temperature and additives on the interaction of ciprofloxacin hydrochloride drug with polyvinylpyrrolidone and bovine serum albumin: spectroscopic and molecular docking study, *J. Oleo Sci.* 70 (3) (2021) 397–407, <https://doi.org/10.5650/jos.ess20306>.
- A. Mukhija, N. Kishore, Drug partitioning in individual and mixed micelles and interaction with protein upon delivery form micellar media, *J. Mol. Liquids* 265 (2018) 1–15, <https://doi.org/10.1016/j.molliq.2018.05.107>.
- P. Meena, N. Kishore, Thermodynamic and mechanistic analytical effect of albumin coated gold nanosystems for antibiotic drugs binding and interaction with deoxyribonucleic acid, *J. Mol. Liquids* 339 (2021) 116718–116731, <https://doi.org/10.1016/j.molliq.2021.116718>.
- P.B. Kandagal, S. Ashoka, J. Seetharamappa, S.M.T. Shaikh, Y. Jadegoud, O.B. Ijare, Study of the interaction of an anticancer drug with human and bovine serum albumin: spectroscopic approach, *J. Pharm. Biomed. Anal.* 41 (2) (2006) 393–399, <https://doi.org/10.1016/j.jpba.2005.11.037>.
- O. Duman, S. Tunç, B. Kancı Bozoğlan, Characterization of the binding of metoprolol tartrate and guaifenesin drugs to human serum albumin and human hemoglobin proteins by fluorescence and circular dichroism spectroscopy, *J. Fluoresc.* 23 (4) (2013) 659–669, <https://doi.org/10.1007/s10895-013-1177-y>.
- A. Mallick, S.C. Bera, S. Maiti, N. Chattopadhyay, Fluorometric investigation of interaction of 3-acetyl-4-oxo-6,7-dihydro-12H indolo-[2,3-a] quinolizine with bovine serum albumin, *Biophys. Chem.* 112 (1) (2004) 9–14, <https://doi.org/10.1016/j.bpc.2004.06.009>.
- S.-F. Sun, B.o. Zhou, H.-N. Hou, Y.i. Liu, G.-Y. Xiang, Studies on the interaction between Oxaprozin-E and bovine serum albumin by spectroscopic methods, *Int. J. Biol. Macromol.* 39 (4-5) (2006) 197–200, <https://doi.org/10.1016/j.ijbiomac.2006.03.020>.
- X.M. He, D.C. Carter, Atomic structure and chemistry of human serum albumin, *Nature* 358 (6383) (1992) 209–215, <https://doi.org/10.1038/358209a0>.
- A. Chandrasekaran, L. Shen, S. Lockhead, A. Oganessian, J. Wang, J. Scatina, Reversible covalent binding of neratinib to human serum albumin in vitro, *Drug Metab. Lett.* 4 (2010) 220–227, <https://doi.org/10.2174/187231210792928206>.
- N.A. Alsaif, T.A. Wani, A.H. Bakheit, S. Zargar, Multi-spectroscopic investigation, molecular docking and molecular dynamic simulation of competitive interactions between flavonoids (quercetin and rutin) and sorafenib for binding to human serum albumin, *Int. J. Biol. Macromol.* 165 (2020) 2451–2461, <https://doi.org/10.1016/j.ijbiomac.2020.10.098>.
- Q. Huang, A.P. Zhang, J. Hao, M.D. Zheng, J.Y. Yang, H.S. Mao, Study on the interaction of ephedrine hydrochloride and pseudoephedrine hydrochloride with human serum albumin by spectroscopy, *J. Anal. Sci.* 4 (2011) 010, https://en.cnki.com.cn/Article_en/CJFDTotal-FXKX201104010.htm.
- B. Guo, Z. Xia, G. Chen, Y. Yin, H. Xu, Study on the interaction of ephedrine, caffeine and acetaminophen with bovine serum albumin by capillary electrophoresis with partial filling technique, *Chin. J. Chromatogr.* 21 (2003) 367–370, https://en.cnki.com.cn/Article_en/CJFDTotal-SPZZ200304015.htm.
- A.E. Till, L.Z. Benet, Renal excretion of pseudoephedrine in the rat, *J. Pharmacol. Exp. Ther.* 211 (1979) 555–560, <https://jpet.aspetjournals.org/content/211/3/555.short>.
- J.u. Yang, D.S. Hage, Chiral separations in capillary electrophoresis using human serum albumin as a buffer additive, *Anal. Chem.* 66 (17) (1994) 2719–2725, <https://doi.org/10.1021/ac00089a019>.
- N. Ye, X. Gu, G. Luo, Chiral separation of ephedrine isomers by capillary electrophoresis using bovine serum albumin as a buffer additive, *J. Chromatogr. Sci.* 45 (5) (2007) 246–250, <https://doi.org/10.1093/chromsci/45.5.246>.
- M. Volpp, U. Holzgrabe, Determination of plasma protein binding for sympathomimetic drugs by means of ultrafiltration, *Eur. J. Pharm. Sci.* 127 (2019) 175–184, <https://doi.org/10.1016/j.ejps.2018.10.027>.
- G.J. Zhang, B. Keita, C.T. Craescu, S. Miron, P.D. Oliveira, L. Nadjio, Polyoxometalate binding to human serum albumin: a thermodynamic and spectroscopic approach, *J. Phys. Chem. B* 111 (2007) 11253–11259, <https://doi.org/10.1021/jp072947u>.
- S. Roy, R.K. Nandi, S. Ganai, K.C. Majumdar, T.K. Das, Binding interaction of phosphorus heterocycles with bovine serum albumin: a biochemical study, *J. Pharm. Anal.* 7 (1) (2017) 19–26, <https://doi.org/10.1016/j.jpba.2016.05.009>.
- P.D. Ross, S. Subramanian, Thermodynamics of protein association reactions: forces contributing to stability, *Biochemistry* 20 (11) (1981) 3096–3102, <https://doi.org/10.1021/bi00514a017>.
- A. Chakrabarty, A. Mallick, B. Haldar, P. Das, N. Chattopadhyay, Binding interaction of a biological photosensitizer with serum albumins: a biophysical study, *Biomacromolecules* 8 (2007) 920–927, <https://doi.org/10.1021/bm061084s>.
- Y.-J. Hu, Y.i. Liu, X.-H. Xiao, Investigation of the interaction between berberine and human serum albumin, *Biomacromolecules* 10 (3) (2009) 517–521, <https://doi.org/10.1021/bm801120k>.
- Z. Chi, R. Liu, Phenotypic characterization of the binding of tetracycline to human serum albumin, *Biomacromolecules* 12 (1) (2011) 203–209, <https://doi.org/10.1021/bm1011568>.
- U. Kragh-Hansen, Molecular aspects of ligand binding to serum albumin, *Pharmacol. Rev.* 33 (1981) 17–53, <https://pharmrev.aspetjournals.org/content/33/1/17.long>.
- J. Wang, C. Xiang, F.F. Tian, Z.Q. Xu, F.L. Jiang, Y. Liu, Investigating the interactions of a novel anticancer delocalized lipophilic cation and its precursor compound with human serum albumin, *RSC Adv.* 4 (2014) 18205–18216, <https://doi.org/10.1039/C3RA46997B>.
- J. Zhang, R. Li, F.L. Jiang, B. Zhou, Q.Y. Luo, Q.L.Y. Yu, X.L. Han, Y. Lin, H. He, Y. Liu, Y.L. Wang, An electrochemical and surface plasmon resonance study of adsorption actions of DNA by *Escherichia coli*, *Colloids Surf. B* 117 (2014) 68–74, <https://doi.org/10.1016/j.colsurfb.2014.01.041>.
- S. Huang, F. Zhu, Q.i. Xiao, Q. Zhou, W. Su, H. Qiu, B. Hu, J. Sheng, C. Huang, Combined spectroscopy and cyclic voltammetry investigates the interaction between [(η⁶-p-cymene) Ru (benzaldehyde-N (4)-phenylthiosemicarbazone) Cl] Cl anticancer drug and human serum albumin, *RSC Adv.* 4 (68) (2014) 36286–36300, <https://doi.org/10.1039/C4RA06083K>.
- Q. WANG, N. Li, W. WANG, Electroanalytical response of dopamine at a metallothioneins self-assembled gold electrode, *Anal. Sci.* 18 (6) (2002) 635–639, <https://doi.org/10.2116/analsci.18.635>.
- F. Qu, N.Q. Li, Y.Y. Jiang, Electrochemical studies of NiTMPyP and interaction with DNA, *Talanta* 45 (1998) 787–793, [https://doi.org/10.1016/S0039-9140\(97\)00154-9](https://doi.org/10.1016/S0039-9140(97)00154-9).
- F. Wang, Y. Xu, J. Zhao, S. Hu, Electrochemical oxidation of morin and interaction with DNA, *Bioelectrochemistry* 70 (2) (2007) 356–362, <https://doi.org/10.1016/j.bioelectchem.2006.05.003>.
- A.J. Bard, L.R. Faulkner, *Electrochemical Methods Fundamentals and Applications*, second ed., John Wiley and sons, New York, 2001.
- C.G. Chilom, M. Bacalum, M.M. Stanescu, M. Florescu, Insight into the interaction of human serum albumin with folic acid: a biophysical study, *Spectrochim. Acta A Mol. Biomol. Spectrosc.* 204 (2018) 648–656, <https://doi.org/10.1016/j.saa.2018.06.093>.
- M.B. Bolattin, S.T. Nandibewoor, S.D. Joshi, S.R. Dixit, S.A. Chimatadar, Interaction of hydralazine with human serum albumin and effect of β-cyclodextrin on binding: insights from spectroscopic and molecular docking techniques, *Ind. Eng. Chem. Res.* 55 (19) (2016) 5454–5464, <https://doi.org/10.1021/acs.iecr.6b00517>.
- M. Sasmal, A.S.M. Islam, R. Bhowmick, D. Maiti, A. Dutta, M. Ali, Site-Selective interaction of human serum albumin with 4-Chloro-7-nitro-1, 2, 3-benzoxadiazole modified olanzapine derivative and effect of β-cyclodextrin on binding: in the light of spectroscopy and molecular docking, *ACS Appl. Bio*

- Mater. 2 (8) (2019) 3551–3561, <https://doi.org/10.1021/acsabm.9b00429>[10.1021/acsabm.9b00429.s001](https://doi.org/10.1021/acsabm.9b00429.s001).
- [42] R.R. Zhang, J.J. Grudzinski, T.I. Mehta, R.R. Burnette, R. Hernandez, P.A. Clark, J. A. Lubin, A.N. Pinchuk, J. Jeffrey, M. Longino, J.S. Kuo, J.P. Weichert, In silico docking of alkylphosphocholine analogs to human serum albumin predicts partitioning and pharmacokinetics, *Mol. Pharm.* 16 (8) (2019) 3350–3360, <https://doi.org/10.1021/acs.molpharmaceut.8b01301>.
- [43] M.A. Bratty, Spectroscopic and molecular docking studies for characterizing binding mechanism and conformational changes of human serum albumin upon interaction with Telmisartan, *Saudi Pharm. J.* 28 (2020) 729–736, <https://doi.org/10.1016/j.jsps.2020.04.015>.
- [44] Y.K. Dijiba, A. Zhang, T.M. Niemczyk, Determinations of ephedrine in mixtures of ephedrine and pseudoephedrine using diffuse reflectance infrared spectroscopy, *Int. J. Pharm.* 289 (1–2) (2005) 39–49, <https://doi.org/10.1016/j.ijpharm.2004.09.027>.
- [45] A.I. Ivanov, R.G. Zhabankov, E.A. Korolenko, E.V. Korolik, L.A. Meleshchenko, M. Marchewka, H. Ratajczak, Infrared and Raman spectroscopic studies of the structure of human serum albumin under various ligand loads, *J. Appl. Spectrosc.* 60 (1994) 305–309, <https://doi.org/10.1007/BF02606317>.
- [46] D. Usoltsev, V. Sitnikova, A. Kajava, M. Uspenskaya, Systematic FTIR spectroscopy study of the secondary structure changes in human serum albumin under various denaturation conditions, *Biomolecules* 8 (2019) 359–376, <https://doi.org/10.3390/biom9080359>.
- [47] R. Yang, H.-J. Zeng, J.-J. Li, Y. Zhang, S.-J. Li, L.-B. Qu, Capillary electrophoresis coupled with end-column electrochemiluminescence for the determination of ephedrine in human urine, and a study of its interactions with three proteins, *Luminescence* 26 (5) (2011) 374–379, <https://doi.org/10.1002/bio.v26.510.1002/bio.1336>.